A Comparative Study of the Bonding Character in the P_4O_n ($n = 6-10$) Series by Means of a Vibrational Analysis

A. R. S. Valentim, B. Engels,* and S. D. Peyerimhoff

Institut für Physikalische und Theoretische Chemie, Universität Bonn, Wegelerstrasse 12, 53115 Bonn, Germany

J. Clade and M. Jansen

Institut für Anorganische Chemie, Universität Bonn, Gerhard-Domagk-Strasse 1, 53121 Bonn, Germany

Received: December 17, 1997; In Final Form: March 5, 1998

In the present work the bonding situation within the P_4O_n ($n = 6-10$) series is studied using a combination of experimental and theoretical vibrational analysis. A correlation between the spectra of the compounds is undertaken, and the shifts of the vibrational frequencies within the series are analyzed. Our study shows that the frequencies of the most modes involving cage motions increase, when more oxygen atoms are added to the phosphorus centers. This reflects the reinforcement of the cage bonds along the P_4O_n ($n = 6-10$) series. For a few bands the frequencies decrease within the series, and this fact results from the reduced masses, which become larger with the increasing number of the substituents.

I. Introduction

The investigation of systematic changes in bonding properties within a series of specially tailored compounds is helpful for the understanding of the relationship between molecular geometries and chemical bonding. The phosphorus oxides P_4O_n ($n = 6-10$) are a suitable example for such studies because this series of compounds is formally obtained by adding terminal oxygen atoms to the phosphorus atoms of the adamantane-like P_4O_6 cage. As a consequence, gradual changes in the bonding properties are expected within this series.

The gradual change in the P−O bond strengths of the P_4O_6 cage is supported by X-ray structure analyses[1−5] which show a stepwise contraction of the P_4O_6 cage when going from P_4O_6 to P_4O_{10}. This contraction is explained by the increase of the bond strengths of the P−O cage bonds due to the larger number of terminally bonded oxygen atoms. Theoretical calculations[6] performed for P_4O_6X considering several different substituents X showed that the changes in the P−O cage bond lengths can be described in terms of the amount of charge being transferred from the pentavalent phosphorus center to the substituent.

Besides X-ray analysis, vibrational spectroscopy is another important tool to elucidate the bonding situation of a molecule because the harmonic vibrational frequencies are directly connected with the force fields of the molecules. Using a combination of theoretical and experimental vibrational spectroscopy, we were able to study the changes in the bonding situations of the series $P_4O_6X_m$ (X = O, S, Se; $m = 1,2$).[7,3]

This combination was crucial because only the theoretical description of the nuclear motions in the various modes could enable a reliable assignment of the experimental spectra, in particular, a correlation of vibrational bands from one spectrum to the other in this series of compounds.

Using the same approach we want to examine, in the present paper, the variations in the bonding situation within the series P_4O_n ($n = 6-10$). Besides the effects already discussed in the study of the P_4O_6X (X = O, S, Se) series, namely, the effect of the heavier masses of the substituents S and Se and the changes of the strength of the P_4O_6 cage bonds, two additional effects must be considered in the present work in order to explain the changes in the vibrational spectra among the series P_4O_n ($n = 6-10$). First, due to the increasing number of oxygen atoms in the series, additional vibrations occur which cause further bands in the spectra or, due to the coupling with cage modes, could also change the entire spectra markedly. The couplings between the vibrations connected with the motions of the substituents and those of the cage atoms could lead to large frequency shifts of the P_4O_6 cage vibrations, and in this case the shifts do not result from changes in the bonding situation of the P_4O_6 cage. Second, the symmetry of the molecules in the P_4O_n ($n = 6-10$) series changes in the order $T_d - C_{3v} - C_{2v} - C_{3v} - T_d$. Therefore, modes which are degenerate for P_4O_6 and P_4O_{10}, are split in the vibrational spectra of the molecules possessing lower symmetries. Furthermore, due to the lower symmetry, more vibrations become IR and Raman active and are allowed to couple with each other.

Experimental IR and Raman spectra[3,8−11] are known for P_4O_n ($n = 6-8,10$). An assignment of the vibrational bands of P_4O_6 and P_4O_{10} has been given by Chapman,[8] while the vibrational spectrum of P_4O_7 was assigned by Moebs and Jansen.[9] Moebs and Jansen also compared the spectra of P_4O_6, P_4O_7, and P_4O_{10} to some extent, but new calculations performed by Mowrey et al.[13] and by us showed that some of their assignments of the spectra of P_4O_6 and P_4O_7 must be corrected, since the correlation in ref 9 was based only on symmetry considerations and not on nuclear displacements. The spectrum of P_4O_8 was assigned only recently.[3] Vibrational data for various phosphorus oxides were also given by Mielke and Andrews,[10] who recorded matrix infrared spectra. On the basis of MNDO/H calculations, Slivko and Krivovyazov[14−18] computed the vibrational spectra of P_4O_n ($n = 6-10$). Since this semiempirical approximation does not

* To whom correspondence should be addressed. E-mail: bernd@thch.uni-bonn.de. FAX: (0228) 73-9066.

S1089-5639(98)00561-1 CCC: $15.00 © 1998 American Chemical Society
Published on Web 05/06/1998

TABLE 1: Bond Lengths (Å) in Phosphorus Oxides[a]

	P_4O_6		P_4O_7		P_4O_8		P_4O_9		P_4O_{10}	
bonds	exptl	theor	exptl	theor	exptl	theor	exptl	theor	exptl	theor
$P^{(III)}-O_a$	1.653	1.648	1.640	1.647	1.627	1.645				
$P^{(III)}-O_b$			1.680	1.662	1.678	1.660	1.675	1.659		
$P^{(V)}-O_b$			1.590	1.601	1.580	1.600	1.573	1.599		
$P^{(V)}-O_c$					1.609	1.611	1.608	1.609	1.599	1.608
$P^{(V)}-O_d$			1.450	1.434	1.455	1.430	1.443	1.427	1.441	1.424

[a] All theoretical values are obtained from a HF/DZP geometry optimization.[3,6] The experimental data are X-ray data given in a review by Clade et al.[12] Experimental structural data of P_4O_8 are taken from ref 3.

describe the alternate shortening and lengthening of the P−O cage bonds upon substitution, and since the authors did not use the correct assignments in fitting their computed data to the experimental spectra, their study needs a revision. The P_4O_9 spectrum has not been discussed by means of ab initio calculations so far.

In the following we will present a thorough comparison of the vibrational spectra of the P_4O_n ($n = 6-10$) series in order to analyze the changes in the bonding properties of the P_4O_6 cage within this series. New calculated and experimentally obtained data will also be introduced.

2. Technical Details

In the present work we used the theoretical methods already employed in our previous studies.[7,3] In a first step, the molecular geometries of the P_4O_n ($n = 6-10$) molecules were optimized using the SCF procedure employing a DZP basis set given by Huzinaga.[19] Then the vibrational frequencies and IR and Raman intensities were calculated at the optimized geometry employing the SCF procedure. To correct errors of the Hartree−Fock force field, the frequencies were scaled employing the scaled quantum mechanical (SQM) force field technique as proposed by Pulay.[21] For the scaling of the force constants the program SCALE[22] was employed. The scale factors were obtained by a least-squares fit to experimental data of P_4O_6, P_4O_7, and P_4O_{10}. For the calculations of the P_4O_n ($n = 6-10$) frequencies, we used averaged scaling factors obtained from the fits for P_4O_6, P_4O_7, and P_4O_{10} (i.e., for consistency all spectra were computed with the same set of scaling factors). Consequently, the results presented in this work deviate to some extent ($\approx$10 cm^{-1}) from the data given in ref 3, where we used scaling factors which were optmized for P_4O_8. Because the accuracy of the SQM force field technique depends strongly on the reliability of the assignments of the vibrational spectra, for P_4O_6 and P_4O_7 the frequencies were calculated in addition using the density functional approach (B3LYP functional) in combination with the DZP basis set mentioned above and furthermore, with a larger basis set which includes a triple-ζ sp part augmented with two polarization functions (TZ2P). This basis was taken from.[20] All calculations were performed with the GAUSSIAN94 code.[23] Descriptions of the nuclear displacements in the various modes were obtained using animations of the program MOLDEN.[24]

The experimental vibrational spectra of P_4O_6, P_4O_7, P_4O_8, and P_4O_{10} were discussed earlier,[3,9] and some experimental vibrational frequencies of P_4O_9 have briefly been reported.[12] In the present work additional IR measurements were recorded for P_4O_6 using a Bruker IFS 113v spectrometer, and a Bruker RFS 100 Raman interferometer was used for the Raman measurements. Raman polarization measurements were performed for liquid P_4O_6. For P_4O_7, the Raman polarization data given by Moebs[9] were checked by newly performig measurements using a single crystal of P_4O_7. The present IR and Raman measurements for P_4O_9 are the most extensive known so far.

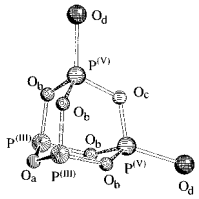

Figure 1. Molecular structure of P_4O_8; schematic illustration of the different P−O bonds. The four different bonds (within C_{2v} symmetry) are specified by different shadings.

3. Results and Discussion

To explain the nomenclature used in the present paper, Figure 1 shows the molecular structure of P_4O_8, and the legend gives a summary of the abbreviations used in the text. A comparison between the experimental and the theoretical geometrical parameters for the various phosphorus oxide molecules is given in Table 1. As shown in previous studies, the geometries optimized with the HF/DZP method are in good agreement with the structures obtained by X-ray diffraction methods,[1−5] the deviations between the theoretical and experimental bond lengths being approximately 2 pm.

3.1. Theoretical and Experimental Frequencies. The vibrational frequencies of the P_4O_n ($n = 6-10$) molecules obtained from the various measurements and calculations are collected in Tables 2−7. Table 2 allows an insight into the accuracy of the computed frequencies. It contains frequencies obtained at the HF/DZP and DFT/TZ2P levels for P_4O_6 together with the values which are given by the SQM method (scaled frequencies). The frequencies obtained in the Raman experiment presented here are listed for a comparison. A summary of the vibrational frequencies of P_4O_6 given by different authors in the literature is given in Table 3. This table contains also a comparison of the different assignments of the P_4O_6 spectrum.

From Table 2, it is seen that the frequencies computed at the HF/DZP level are about 10% higher than their experimental counterparts. If the DFT/TZ2P method is used, all frequencies go to about 88%−92% of their HF/DZP values, with exception of the $2f_1$ mode which is shifted to about 80% of the HF/DZP values. This strong frequency shift cannot be verified by experimental data, because this mode is inactive in both IR and Raman experiments. For the more sophisticated DFT/TZ2P method, the deviations between the theoretical and experimental values are only 10−20 cm^{-1}. In addition, one can see that, with the exception of the band with the highest frequency, the DFT/TZ2P values are always smaller than the experimental frequencies. The differences between the DFT/TZ2P, HF/DZP, and experimental values are reflected by the calculated bond lengths which are somewhat too short at the HF/DZP level (1.648 Å, exp: 1.653 Å) but somewhat too long at the DFT/TZ2P level (1.662 Å). In general, the accuracy of the scaled frequencies based on the HF/DZP level are similar to those obtained from the DFT/TZ2P computation. Furthermore, the

TABLE 2: Vibrational Frequencies (in cm^{-1}) and Relative Intensities of P_4O_6 from Different Methods in Comparison with Experimental Data

HF/DZP				DFT/TZ2P		scaled		exptl (present)		
Ra	IR	freq	symmetry	IR	freq	IR	freq	Ra	IR	freq
0	0	321	F_1	0	276	0	302		inactive	
10	0	329	E	0	291	0	297	10	v.w.[a]	302
18	4	448	F_2	4	400	4	410	18	v.s.	407
0	0	622	F_2	0	545	0	570			
100	0	680	A_1	0	600	0	597	100,p.		614
55	10	704	F_2	11	626	10	626	55	v.s.	644
5	0	714	E	0	637	0	633			
0	0	736	F_1	0	572	0	645		inactive	
0	0	813	A_1	0	730	0	739			
4	100	1075	F_2	100	931	100	946	5	v.v.s.	921

[a] v.w. = very weak. v.s. = very strong. v.v. = very very strong.

TABLE 3: Vibrational Frequencies of P_4O_6 Obtained from Different Authors in the Literature (Values in cm^{-1})

symmetry	ref 25	ref 8	ref 10	exptl (this work)	scaled (ref 13)
F_1					288.4
		285[a]			
E	305[b]	302[b]		302[b]	300.5
F_2	408	407	405	407	404.6
F_2	562[c]	549[d]			562.8
		569[c]			
A_1	620	613		614	617.7
F_2	642	643	640	644	645.5
E		691			659.3
		702[e]			
F_1					677.6
A_1		718[d]			738.5
F_1		832			
F_2	959	919	953	921	980.8

[a] Assigned as E. [b] Assigned as F_2. [c] Assigned as A_1. [d] Unassigned. [e] Assigned as combination band.

agreement between the DFT/TZ2P and the experimental results shows that the errors given by the HF/DZP method do not result from influences of the agregate state or unharmonic resonance. The computed IR intensities obtained by DFT/TZ2P method also differ slightly from those obtained by the HF/DZP treatment. [Both methods, however, show considerable intensities for the bands marked as "very strong" in the experimental spectra.]

From Table 3 it is seen that there are also uncertaincies in the experimental data. Generally the discrepancies between the various measurements are less than 10 cm^{-1}, but the frequency of the highest and strongest band varies between 919 and 959 cm^{-1} in the various experiments. Some of the previous assignments are different from theory the present work and will be discussed later on. The computed data of Mowrey[13] are very close to the results of the present calculations and in general agree with our assignment.

A comparison of the scaled frequencies obtained for P_4O_7 with those given by two measurements[9,26] is given in Table 4. The dependency of the P_4O_7 frequencies on the theoretical method has recently been discussed[27] and is very similar to our findings for P_4O_6. However, because bands at higher frequencies are experimentally known for P_4O_7, these could be incorporated into the scaling procedure, which is then adequate up to higher frequencies than for P_4O_6. Again it is seen that different experimental conditions yield values which differ up to 10 cm^{-1} in the low-frequency and up to 30 cm^{-1} in the high-frequency range.

The general trends in the theoretical and experimental frequencies for P_4O_8, P_4O_9, and P_4O_{10} are similar to what has been observed for P_4O_6 and P_4O_7. Larger differences are always seen for the higher frequency parts of the spectra, and noticeable discrepancies are also present between the two experimental studies of P_4O_8[3,10] (Table 5). For P_4O_{10}, the two theoretical results vary by less than 20 cm^{-1}; the assignment of the bands is the same in all investigations (Table 7).

TABLE 4: Comparison of the Calculated Vibrational Frequencies of P_4O_7 with Experimental Data (Values in cm^{-1})

		ref 26		ref 9		this work
symmetry	scaled	IR	Raman	IR	cryst. IR	Raman
E	262		261		266−277	269
A_2	288					
E	297		303		299[a]	306
E	342				323	333
A_1	382		388		392[b]	392
E	423		425	424	427[c]	429
A_1	546		528	534	532	534
E	568					
A_1	595	627	624	629	615	625
A_1	619				635[d]	
E	626		651		653	
A_2	648					
E	708	695	709		711	708
E	732					
A_1	724					
A_1	942		928	945	935	930
E	958	955	958	966	965	960
A_1	1357	1362	1328	1364	1345	1333

[a] Assigned as A_1. [b] Assigned as E. [c] Assigned as A_1. [d] Assigned as combination band.

3.2. Comparison of the Vibrational Spectra of the P_4O_n (n = 6−10) Series. The comparison of the vibrational frequencies of the molecules P_4O_n (n = 6−10) are based on the computed frequencies, which are obtained with the SQM force field technique in connection with experimental IR and Raman results.

The first (P_4O_6) and the last (P_4O_{10}) member of the P_4O_n (n = 6−10) series are built of four equivalent PO_3 and O=PO_3 units, respectively. A good description for a vibrational mode is therefore obtained when the vibrations are discussed in terms of linear combinations of the nuclear displacements within these subunits. This is done in Table 8 which gives a correlation of the vibrational bands within the P_4O_n (n = 6−10) series together with short descriptions of the nuclear motions. For several modes, the nuclear motions are also indicated in Figure 2. Further information, including pictures or animations of the nuclear motions can be obtained from the authors upon request. For the molecules P_4O_n (n = 7−9) the descriptions of the nuclear motions are less obvious because the lower symmetry

TABLE 5: Vibrational Frequencies of P_4O_8 (Values in cm^{-1}) Obtained from Different Methods

		ref 3		
symmetry	scaled	IR	Ra	ref 10
A_2	259		260	
A_1	265		267	
B_1	266		270	
B_2	267			
A_2	297		302	
A_1	307		310	
B_1	320		317	
A_2	364			
B_2	375			
B_2	399		396	
A_1	402	412	415	440
B_1	432	434	436	
A_1	553	552	556	556
B_2	567			614
B_1	572			
A_1	590	602	606	
A_1	623	636	642	683
B_2	665	660	658	
B_1	691	675		
A_1	714	702	700	
A_2	727			
B_1	729			
A_1	736			
A_2	775			
B_2	792	782		
B_2	959	963		
A_1	970			996
B_1	972	979		1004
B_2	1359	1357	1336	1385
A_1	1377	1364	1358	1402

TABLE 6: Vibrational Frequencies (in cm^{-1}) and Relative Intensities of P_4O_9

	scaled			exptl			
				IR		Ra	
symmetry	freq	IR	Ra				
E	259	0	13			259.5	v.s.
E	269	1	6	267	v.s.[e]	263	s.
A_2	271	0	0				
A_1	275	2	6	281	v.s.	283	m.
E	311	0	1	317	w.	320	w.
E	372	0	3	362	w.	357	?
E	394	2	22	407	s.	403	v.s.
A_2	423	0	0	423(?)	s.	413(?)	w.
A_1	432	5	22	431	v.s.	433	s.
?				487[a]	m, br.		
A_1	548	2	73	559	v.s., br.	570	v.s.
E	573	1	2	589	m.	596	v.s.
A_1	586	1	14	609	m.	608	m.
?						631[b]	v.w.
E	691	6	6	657	v.s., br.	672	v.w.
A_1	711	21	37	715	w.	698	s.
E	751	5	0	751	s.		
A_1	771	8	2	777	v.s.		
E	797	9	5				
A_2	831	0	0				
A_1	975	100	0	1000	v.s., br.		
E	994	69	0				
E	1372	54	26	1379	v.s., br.	1362	m.
A_1	1397	11	100			1392	s.
?				1621[c]	w.		
?				1691[d]	w.		

[a] Combination band: 751 ($6A_1$) − 267 ($1A_1$) = 484. [b] First overtone of 3E (640). [c] Combination band: 1362 (11E) + 259 (1E) = 1621. [d] Combination band: 1362 (11E) + 320 (3E) = 1682. [e] br. = broad. m. = medium. s. = strong. v.s. = very strong. w. = weak.

of these molecules leads to an enhanced coupling between various vibrations.

a. Vibrational Modes Involving the $P^V{=}O_d$ Displacements.

TABLE 7: Comparison of Theoretical Vibrational Frequencies of P_4O_{10} (Values in cm^{-1}) with the Experimental Data

		ref	ref	ref	ref	ref	refs
symmetry	scaled	13	25	28	8	10	29 and 30
E	256	243.8	254		258		257
F_2	278	263.2	264	270	278		278
F_1	270	261.1					
E	321	331.7					330
F_1	426	410.4					
F_2	400	406.0	411	409	424	412	424
A_1	528	539.5	553		556		
F_2	581	590.2		575	573		573
A_1	721	749.4	717		721		721
F_2	767	777.5		764	760	767	764
E	811	830.3					
F_1	832	872.0					
F_2	1013	1049		1012	1010	1025	1015
F_2	1382	1397	1406	1404	1390	1408	1386
A_1	1415	1429	1440		1413		1417

Formally the vibrational modes of the molecules P_4O_n ($n = 6-10$) can be constructed by combining the P_4O_6 cage vibrations with the additional vibrations involving the $P^V{=}O_d$ groups. Both can be divided into bending and stretching vibrations, respectively. Let us first consider the variations within the series P_4O_n ($n = 6-10$) which arise from the $P^V{=}O_d$ displacements. While the bending vibrations which involve motions of the $P^V{=}O_d$ bonds occur in the low-frequency region of the spectra (up to approximately 300 cm^{-1}), the $P^V{=}O_d$ stretching vibrations are located about 300−400 cm^{-1} above the highest cage vibration. The cage vibrations occur between 300 and 1000 cm^{-1} (Tables 3−8). As discussed for P_4O_7 and P_4O_8,[3,7] the $P^V{=}O_d$ bonds are much stronger than the P−O cage bonds, so that a coupling between the cage modes and the $P^V{=}O_d$ stretching vibrations is not found. If one considers the multiple substituted compounds, the normal modes which result from linear combinations of stretching vibrations of the $P^V{=}O_d$ units are split into a symmetric a_1 and one further mode, which possesses b_2 symmetry for P_4O_8, e symmetry for P_4O_9, and f_2 symmetry for P_4O_{10}. In the a_1 vibration, all $P^V{=}O_d$ units move in phase; the antisymmetric combination of the $P^V{=}O_d$ stretching displacements appears at lower frequencies. The splitting between the symmetric and antisymmetric combinations increases from about 20 cm^{-1} for P_4O_8 to approximately 30 cm^{-1} for P_4O_{10}. The frequencies of both modes increase along the series, the frequency shift of the a_1 mode being more pronounced (58 cm^{-1}) than that of the second mode (23 cm^{-1}).

The modes which involve the bending of the $P^V{=}O_d$ units form the lower frequency range of the spectra. For P_4O_{10}, the two lowest modes (1e at 256 cm^{-1} and $1f_2$ at 278 cm^{-1}) consist of pure bending motions of the $P^V{=}O_d$ units. The higher lying bending modes of the $P^V{=}O_d$ units are related to the $1f_1$ cage mode of P_4O_6 (302 cm^{-1}). The nuclear motion connected with this mode represents a libration motion of one PO_3 unit against the rest of the molecule. A comparison of the nuclear motions of P_4O_6 and P_4O_{10} shows that in P_4O_{10} both the $1f_1$ mode (calculated at 270 cm^1) and the $2f_1$ mode (calculated at 426 cm^{-1}) must be correlated with the mode f_1 of P_4O_6 and can be described as a mixture of this libration motion with the bending motions of the $P^V{=}O_d$ units. This contribution of bending vibrations of the terminal $P^V{=}O_d$ units explains the energy shift of the $1f_1$ mode from 302 cm^{-1} in P_4O_6 to 270 cm^{-1} for P_4O_{10}. The relatively high frequency of the $2f_1$ mode of P_4O_{10} is a result from contributions of O−P−O bending motions of the cage (i.e., neither shift does result from changes in the bonding situation of the cage). Because of the low symmetry, contribu-

TABLE 8: Comparison of the Vibrational Spectra (Values in cm^{-1})

modes description	P_4O_6	P_4O_7	P_4O_8	P_4O_9	P_4O_{10}
symmetric bending of $P^V{=}O_d$ bonds		1 e 262	1 a_1 259	1 e 259	1 e 256
			1 a_2 265		
symmetric bending of 3 $P^V{=}O_d$ bonds				1 a_1 275	1 f_2 278
bending motion of $P^V{=}O_d$ with contributions of the libration motion (see Figure 2)			1 b_1 266	2 e 269	2 f_1 426
			1 b_2 267	1 a_2 271	
libration motion of PO_3 respectively $O{=}PO_3$ units (see Figure 2)	1 f_1 302	1 a_2 288	2 b_1 320	4 e 372	1 f_1 270
		3 e 342	3 a_2 364	2 a_2 423	
			2 b_2 375		
symmetric bending of P−O−P cage bonds	1 e 298	2 e 297	2 a_1 307	3 e 311	2 e 321
			2 a_2 297		
umbrella motion of PO_3 respectively $O{=}PO_3$ units (see Figure 2)	1 f_2 410	1 a_1 382	3 a_1 402	5 e 394	2 f_2 400
		4 e 423	3 b_2 399	2 a_1 432	
			3 b_1 432		
symmetric bending motion of $O{-}P^V{-}O$ cage bond (see Figure 2)	2 f_2 570	2 a_1 546	4 a_1 553	6 e 573	3 f_2 581
		5 e 568	4 b_2 567	4 a_1 586	
			4 b_1 572		
cage breathing mode	1 a_1 597	3 a_1 595	5 a_1 590	3 a_1 548	1 a_1 528
stretch motion (see Figure 2)	3 f_2 626	4 a_1 619	6 a_1 623	7 e 691	4 f_2 767
		6 e 626	5 b_2 665	6 a_1 771	
			5 b_1 691		
antisymmetric stretching of PO_3 and $O{=}P$ O_3 units respectively (see Figure 2)	2 e 633	8 e 732	8 a_1 736	9 e 797	3 e 811
			5 a_2 775		
similar to the 2 e mode of P_4O_6 (see Figure 2)	2 f_1 645	2 a_2 648	6 b_1 729	8 e 751	3 f_1 832
		7 e 708	4 a_2 727	3 a_2 831	
			6 b_2 792		
umbrella mode (see Figure 2)	2 a_1 739	5 a_1 724	7 a_1 714	5 a_1 711	2 a_1 721
symmetric stretch (ν_s) in PO_3 and $O{=}PO_3$ units, respectively (see Figure 2)	4 f_2 946	6 a_1 942	9 a_1 959	10 e 994	5 f_2 1013
		9 e 958	7 b_2 972	7 a_1 975	
			7 b_1 970		
negative linear combination of stretching of $P^V{=}O_d$			8 b_2 1359	11e 1372	6 f_2 1382
positive linear combination of stretching of $P^V{=}O_d$		7 a_1 1357	10 a_1 1377	8 a_1 1397	3 a_1 1415

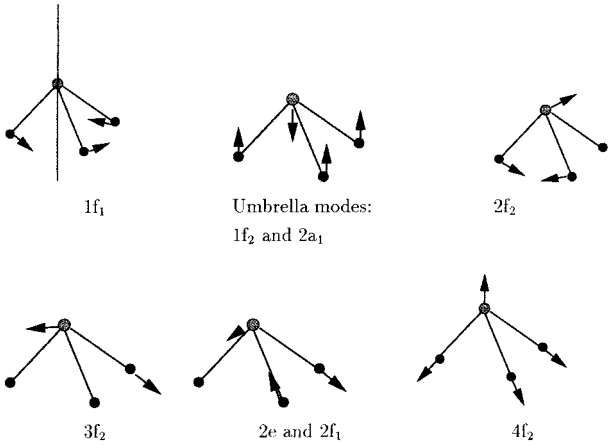

Figure 2. Pictorial representation of the vibrational modes of the $P{-}O_3$ unit of P_4O_6 cage structure.

tions of the above-discussed libration mode to all $P^V{=}O_d$ vibrations are found for P_4O_7, P_4O_8, and P_4O_9. However, a precise analysis of the amounts of these contributions is very difficult due to the low symmetry of the P_4O_n ($n = 7-9$) molecules.

b. P_4O_6 Cage Modes. The modes which are correlated with the 1e mode of P_4O_6 (at 298 cm^{-1}) appear at 297 cm^{-1} for P_4O_7 (2e), at 307 cm^{-1} and at 297 cm^{-1} for P_4O_8 ($2a_1$ and $2a_2$, respectively), at 311 cm^{-1} for P_4O_9 (3e), and at 321 cm^{-1} for P_4O_{10} (2e). They correspond to $O{-}P{-}O$ bending vibrations of the P_4O_6 cage. Since only negligible contributions of the displacements of the $P^V{=}O_d$ units to these modes are found, an increase of the frequencies of these modes can be observed when going from P_4O_6 to P_4O_{10}. This is the first evidence of a reinforcement of the cage bonds along the series of compounds under consideration.

Assigning the band at 298 cm^{-1} in P_4O_6 to an 1e mode, we obtain a consistent correlation with the low energy bands of the P_4O_n ($n = 7-10$) spectra. This is not the case if one follows the assignment suggested by Chapman[8] (which is followed by Moebs[9]) who classifies the lowest band as e and characterizes the second (302 cm^{-1} exptl, 307 cm^{-1} calc.) as f_2 (Table 3). On the basis of this assignment one would expect a f_2 cage mode for P_4O_{10}. The calculations show, however, that the only f_2 mode in this energy region of the P_4O_{10} spectrum involves $P^V{=}O_d$ motions. The correlation between the P_4O_6 and P_4O_7 spectra would also not be obvious if one follows the assignment in ref 8. The P_4O_7 assignment of the band at 300 cm^{-1}, which has originally been characterized as an a_1 mode, was corrected[7] to an E type of vibration. Hence the P_4O_7 spectrum does not show any a_1 mode in the low energy part of the spectrum. A mode of this symmetry would have to arise from the splitting of the f_2 mode (which appears in Chapman's assignment of P_4O_6[8]) when going to the P_4O_7 molecule which possesses a lower symmetry. In this context it is also important to note that in the P_4O_9 molecule there is only one vibration with A_1 symmetry below 400 cm^{-1}, but this involves $P^V{=}O_d$ motions. For all these reasons the assignment of the P_4O_6 cage motions and their correlations with the corresponding modes in P_4O_n ($n = 7-10$) seem to be consistent. The splitting of the vibrational levels within the P_4O_n series is plotted in Figure 3.

The $1f_2$ mode of P_4O_6 (410 cm^{-1}) represents an umbrella mode of the PO_3 units. It correlates with the $2f_2$ mode of P_4O_{10} (400 cm^1), which represents an umbrella mode of the $O{=}PO_3$ units. Both appear at similar frequencies ($\approx$400 cm^{-1}). In P_4O_{10}, the respective P^V and O_d centers move as rigid $P^V{=}O_d$ units during the $O{=}PO_3$ umbrella motion. As a result, the reduced mass for the P_4O_{10} vibration is larger than for the P_4O_6 vibration. A simple model that neglects the changes in the bonding situation of the cage in P_4O_6 and P_4O_{10} would therefore predict a lower frequency for P_4O_{10} than for P_4O_6. The similarity of the frequencies of this mode in P_4O_6 and P_4O_{10}

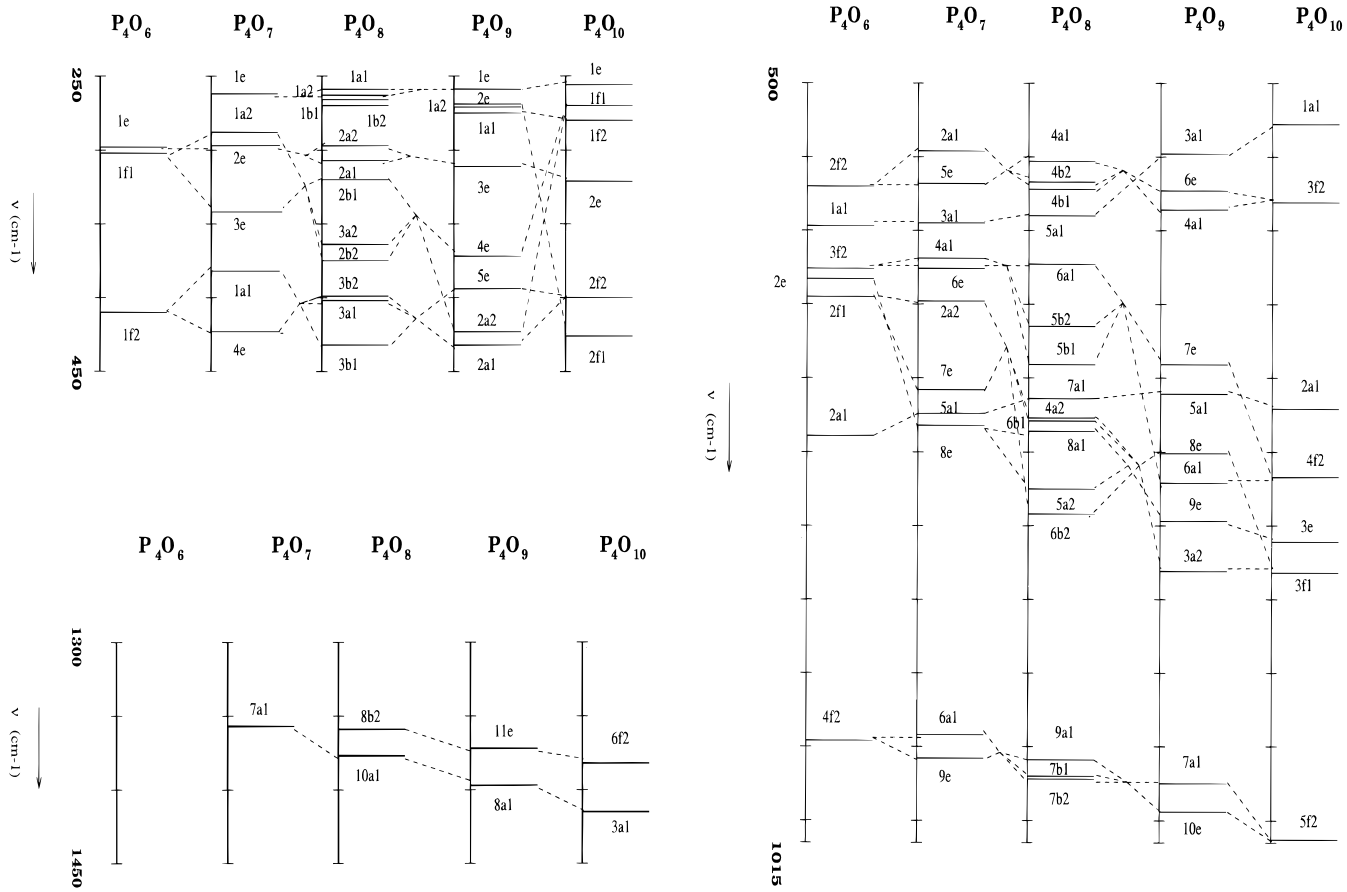

Figure 3. Correlation of the vibrational modes within the P_4O_n ($n = 6-10$) series. (a) lower part of the spectra (250−450), (b) middle part of the spectra (500−1100), (c) upper part of the spectra (1300−1450).

indicates a compensation of the frequency lowering (due to the larger mass) and the increase in frequency (due to the bond strengthening effect within the cage). Similar cancellation effects can be observed for the modes that are connected with the $2f_2$ mode of P_4O_6 (Table 8).

For P_4O_6, Chapman[8] assigned the band at 569 cm^{-1} to an a_1 fundamental (Table 3). As a consequence, considering also the most intense Raman band at 614 cm^{-1} (also A_1 symmetry), his assignment gives two a_1 modes between 550 and 700 cm^{-1}. However, neither the theoretical study of Mowrey et al.[13] nor our calculations can support this assignment. Both computations give only one a_1 fundamental below 600 cm^{-1}, which must be correlated with the most intense Raman band. Therefore, theory suggests that the band found at 569 cm^{-1} is the first overtone of the 285 cm^{-1} fundamental. The new assignment is supported by the P_4O_{10} spectra for which both theory and experiment give only one a_1 fundamental below 700 cm^{-1}. The Raman intensity of this overtone could be perhaps a result from a weak coupling with the most intense Raman band which is found around 620 cm^{-1}.

An alternative explanation for the experimentally found polarized band at 569 cm^{-1} could be a coupling between the a_1 component of the f_2 mode at 570 cm^{-1} and the most intense Raman band (a_1 mode at 614 cm^{-1}). This higher order effect could be enhanced by environment effects, which might lead to symmetry breaking. In this case the intensity of the polarized band at 569 cm^{-1} would result from an intensity borrowing from the most intense Raman band.

The most pronounced effect of nuclear mass (a shift of 70 cm^{-1} to lower frequencies of this band from P_4O_6 to P_4O_{10}) is found in the lowest cage breathing mode (P_4O_6, $1a_1$ at 597 cm^{-1}; P_4O_7, $3a_1$ at 595 cm^{-1}; P_4O_8, $5a_1$ at 590 cm^{-1}; P_4O_9, $3a_1$ at 548 cm^{-1}; P_4O_{10}, $1a_1$ at 528 cm^{-1}), in which the displacements of the P^{III} centers are substituted by the displacements of the entire $P^V{=}O_d$ units when going from P_4O_6 to P_4O_{10}.

The modes in the range from 630 to 660 cm^{-1} for P_4O_6 ($3f_2$ at 626 cm^{-1}, 2e at 633 cm^{-1}, and $2f_1$ at 645 cm^{-1}) correlate with the modes appearing in the range from 770 to 840 cm^{-1} for P_4O_{10} ($4f_2$ at 767 cm^{-1}, 3e at 811 cm^{-1}, $3f_1$ at 832 cm^{-1}). The vibrations of P_4O_7, P_4O_8, and P_4O_9, which are related to these modes are listed in Table 8. All these vibrations represent P−O stretching vibrations within the cages (sketches of the movements taking place in one PO_3 unit are depicted in Figure 2). The strong increase in these frequencies (141, 178, and 187 cm^{-1}, respectively) from P_4O_6 to P_4O_{10} reflects the increasing bond strenghts of the cage bonds. The differences in the increase may result from the number of P−O bonds involved in these modes (see Table 8 and Figure 2).

Differences arising from the participations of P^{III} or P^V are very distinctly seen from the P_4O_8 modes $4a_2$, $6b_1$, and $6b_2$, which correlate with the $2f_1$ mode of P_4O_6 (at 645 cm^{-1}). The mode with the highest frequency ($6b_2$ at 792 cm^{-1}) involves mainly the $O{=}PO_3$ units, while in the $4a_2$ mode (at 727 cm^{-1}) the motions of the PO_3 units dominate. In the mode lying between these two modes ($6b_1$ at 729 cm^{-1}) one PO_3 and one $O{=}PO_3$ unit are involved. The difference between PO_3 and $O{=}PO_3$ units is also obvious from a comparison of P_4O_7 ($2a_2$ at 648 cm^{-1}, 7e at 708 cm^{-1}) with P_4O_9 (8e at 751 cm^{-1}, $3a_2$ at 831 cm^{-1}). In P_4O_7, the $2a_2$ mode (P^V center does not move) appears at a lower frequency than the 7e mode (P^V center moves). For P_4O_9, the opposite sequence is found, because the ratio of the P^{III} and P^V centers is inverted. The small difference

between the frequencies of the $3a_2$ mode of P_4O_9 (at 831 cm^{-1}) and of the $3f_1$ mode of P_4O_{10} (at 832 cm^{-1}) is not surprising, since in the $3a_2$ mode only the O═PO_3 units move.

The modes, which correlate with the $2a_1$ vibration of P_4O_6 (P_4O_7, $5a_1$ at 724 cm^{-1}; P_4O_8, $7a_1$ at 714 cm^{-1}; P_4O_9, $5a_1$ at 711 cm^{-1}; P_4O_{10}, $2a_1$ at 721 cm^{-1}) represent also umbrella motions of the PO_3 and O═PO_3 units, respectively. The slight decrease of the calculated frequencies (17 cm^{-1}) is again a result from a compensation of the mass effect by the strengthening of the cage bonds.

The differences between the frequencies of the $4f_2$ mode of P_4O_6 (946 cm^{-1}) and the $5f_2$ mode of P_4O_{10} (1013 cm^{-1}) again reflect the changes in the bonding situation of the cages in P_4O_6 and P_4O_{10}.

4. Conclusions

In the present work we have studied the changes in the bonding situation within the series P_4O_n ($n = 6-10$) using a combination of theoretical and experimental spectroscopy. The theoretical data were obtained from the scaled force field technique primarily based on HF/DZP calculations, while selected points have also been computed by using DFT(B3LYP)/TZ2P treatments. The experimental data were mainly taken from our earlier work but new data for P_4O_6, P_4O_7, and P_4O_9 were also presented. The vibrational spectra of all P_4O_n ($n = 6-10$) compounds are assigned in the present work on the basis of the calculations, and the relations between them are thoroughly analyzed. The results show that the vibrations, which involve motions of the additional oxygen atoms appear either in the low-energy region or in the high-energy region of the vibrational spectrum. In the low-energy range (below 260 cm^{-1}), all bands correspond to bending motions of the terminal $P^V═O_d$ bonds. In the energy range above 1100 cm^{-1} only stretching vibrations of the terminal $P^V═O_d$ bonds are observed. These bonds are so strong that no coupling of the $P^V═O_d$ stretching motions with the motions of the P−O cage bonds can be found. A coupling between the vibrations of the terminal $P^V═O_d$ units and the P_4O_6 cage modes is only observed for the modes of P_4O_n ($n = 7-10$), which correlate with the $1f_1$ vibration of P_4O_6.

The shift of the bands to higher frequencies within the P_4O_n ($n = 6-10$) series, which is observed in the middle range of the spectrum (300−1000 cm^{-1}) is a clear indication for the increase in the strength of the P−O cage bonds. For two bands, a shift to lower frequencies occurs and the present analysis attributes this effect to the higher reduced mass of the moving units (phosphorus atom for P_4O_6, $P^V═O_d$ for P_4O_{10}).

Acknowledgment. The financial support of the Deutsche Forschungsgemeinshaft (Sonderforschungsbereich 334) is gratefully acknowledged.

References and Notes

(1) Jansen, M.; Voss, M.; Deiseroth, H.-J. *Angew. Chem.* **1981**, *93*, 1023.

(2) Jansen, M., Voss, M. *Angew. Chem.* **1981**, *93*,.

(3) Valentim, A. R. S.; Engels, B.; Peyerimhoff, S. D.; Tellenbach, A.; Strojek, S.; Jansen, M. *Z. Anorg. Allg. Chem.* Submitted for publication.

(4) Jansen, M.; Lüer, B. *Z. Kristallogr.* **1991**, *19*, 247.

(5) Jansen, M.; Lüer, B. *Z. Kristallogr.* **1986**, *17*, 149.

(6) Mühlhäuser, M.; Engels, M.; Marian, C. M.; Peyerimhoff, S. D.; Bruna, P. B.; Jansen, M. *Angew. Chem.* **1994**, *106*, 576.

(7) Valentim, A. R. S.; Engels, B.; Peyerimhoff, S. D.; Clade, J.; Jansen, M. *Inorg. Chem.* **1997**, *36*, 2451.

(8) Chapman, A. C. *Spectrochim. Acta A* **1968**, *24*, 1687.

(9) Jansen, M.; Moebs, M. *Z. Anorg. Allg. Chem.* **1984**, *514*, 39.

(10) Mielke, Z.; Andrews, L. *J. Phys. Chem.* **1989**, *93*, 2971.

(11) Jansen, M.; Clade, J.; Frick, F. Unpublished results.

(12) Clade, J.; Frick, F.; Jansen, M. *Adv. in Inorg. Chem.* **1994**, *41*, 327.

(13) Mowrey, R. C.; Williams, B. A.; Douglass, C. A. *J. Phys. Chem. A* **1997**, *101*, 5748.

(14) Slivko, S. A.; Krivovyazov, E. L. *Russ. J. Inorg. Chem.* **1993**, *10*, 1606.

(15) Slivko, S. A.; Krivovyazov, E. L. *Russ. J. Inorg. Chem.* **1994**, *39*, 122.

(16) Slivko, S. A.; Krivovyazov, E. L. *Russ. J. Inorg. Chem.* **1994**, *1*, 122.

(17) Slivko, S. A.; Krivovyazov, E. L. *Russ. J. Inorg. Chem.* **1993**, *12*, 1884.

(18) Slivko, S. A.; Krivovyazov, E. L. *Russ. J. Inorg. Chem.* **1993**, *11*, 1740.

(19) Huzinaga, H. *Approximate Atomic Wave functions*; Department of Chemistry Report; University of Alberta, Alberta: Canada, 1965; Vols. I and II.

(20) For phosphorus, see: McLean, A. D.; Chanler, G. S. *J. Chem. Phys.* **1980**, *72*, 5639. For oxygen, see: Huzinaga, H. *Approximate Atomic Wave functions*; Division of Theoretical Chemistry, Department of Chemistry: University of Alberta, 1971; Vols. I and II.

(21) Pulay, P.; Forgarasi, G.; Ponger, G.; Boggs, J. E.; Vargha, A. *J. Am. Chem. Soc.* **1983**, *105*, 7037.

(22) Pulay, P.; et al. TX90; University of Arkansas: Fayetteville, Arkansas, 1990.

(23) Frisch, M. J.; Trucks, G. W.; Schlegel, H. B.; Gill, P. M. W.; Johnson, B. G.; Robb, M. A.; Cheeseman, J. R.; Keith, T.; Petersson, G. A.; Montgomery, J. A.; Raghavachari, K.; Al-Laham, M. A.; Zakrzewski, V. G.; Ortiz, J. V.; Foresman, J. B.; Cioslowski, J.; Stefanov, B. B.; Nanayakkara, A.; Challacombe, M.; Peng, C. P.; Ayala, P. Y.; Chen, W.; Wong, M. W.; Andres, J. L.; Reploge, E. S.; Gomperts, R.; Martin, R. L.; Fox, J. F.; Bincley, J. S.; DeFrees, D. J.; Baker, J.; Stewart, J. J. P.; Pople, J. A. GAUSSIAN94: Gaussian, Inc.: Pittsburgh, PA, 1995.

(24) Schafternaar, G. MOLDEN, CAOS/CAMM; Center Nijmegen: Toernooiveld, Nijmegen, Netherlands, 1991.

(25) Beattie, I. R.; Livingston, K. M. S.; Ozin, G. A.; Reynolds, D. J. *J. Chem. Soc. A* **1970**, *3*, 449.

(26) Walker, M. L., and Mills, J. L. *Synth. React. Inorg. Metal-Org. Chem.* **1975**, *5*, 29.

(27) Valentim, A. R. S.; Engels, B.; Peyerimhoff, S. D.; Clade, J.; Jansen, M. Submitted for publication.

(28) Konings, R. J. M.; Cordfunke, E. H. P.; Booij, A. S. *J. Mol. Spectrosc.* **1992**, *29*, 152.

(29) Zijp, D. H. *Adv. Mol. Spectrosc.* **1962**, *1−3*, 345.

(30) Gerding, H. *J. Chim. Phys.* **1948**, *46*, 118.